EAN 2020
58th conference on experimental stress analysis

Damage Parameters During Thermomechanical Fatigue

PAŘEZ J.

Výzkumný a zkušební letecký ústav, a.s., Czech Aerospace Research Centre;
Beranových 130, 199 05, Prague - Letnany, Czech Republic

parez@vzlu.cz

Keywords: Thermo-mechanical fatigue, Damage parameter, TMF prediction

Abstract. Presented paper deals with damage parameters in prediction of thermomechanical fatigue. The objective of the paper is to compare the input parameters and evaluate the results. Showed thermomechanical fatigue analysis is based by the Nagode calculation with the damage parameter according to the SWT methodology based on the fatigue coefficients and the power relation. Further according to Zamrik's and Ostergren's methodology. Showed methodologies were applied to experimental data, where regression coefficients of respective models were obtained to obtain uniform dependence on the number of half cycles and plots of the damage parameter were plotted.

Introduction

Most methods of predicting fatigue life when considering a combination of thermal and mechanical stress are focused on iso-thermal fatigue, which is characterized by variable mechanical stress of the component in a steady-state temperature field. On the other hand, when the temperature field changes, the stress gradients change due to temperature gradients and during thermal cycling the component is subjected to "thermal fatigue".

A more complicated type is when a component is subjected to a variable temperature field and variable mechanical stress at the same time. One such component is a turbine blade that is under different thermomechanical cycles depending on the blade position. i.e. at the root, leading edge or trailing edge. Thus, there is an interaction of these effects collectively referred to as the "thermo-mechanical fatigue". In general, the time courses of mechanical and thermal stresses can be independent of one another. This type of load typically occurs under different transition modes of thermally stressed machine parts. With regard to turbine engines, these are especially the engine start and stop modes, respectively transition state when operating mode changes, there are two model types of cycles, in-phase (IP) and out-phase (OP).

Variable thermal and mechanical loads may have a much greater damaging effect than mere isothermal stress if improperly combined. Damage, type of damage, eventually its individual modes, which are formed during loading and depend mainly on the type of material and its properties, amplitude and strain rate, temperature and, last but not least, the mutual phase between the course of thermal and mechanical loading. A characteristic feature of TMF is often significant amplitude of plastic deformation, which evokes the problem of low cycle fatigue with life prediction in several thousand cycles.

The following chapters describe the damage parameters and their effect on the prediction of fatigue from mechanical stresses. The methodology of the calculation of thermo-mechanical fatigue was developed within the project to increase the utility properties of the GE H75 turboprop engine with modifications necessary for use in a training aircraft capable of advanced aerobatics. The object of the project is the development of methodology and software for the

prediction of thermo-mechanical fatigue and calculation of damage growth on critical parts. By determining the life of individual critical parts, the knowledge of the whole engine is deepened, individual parts can be structurally optimized and maintenance needs can be appropriately determined. Validation of this method will be used to evaluate the possibility of transitioning from a scheduled maintenance system to an actual condition maintenance system.

Damage parameter

The damage parameter is a parameter quantifying the key fatigue damage control variables. The original damage parameter proposed in the publications, sees for example [3], [5] or [6], is the classic SWT parameter. In addition to this, other parameters are also used for the target area of complex thermo-mechanical stress. The parameters differ in the consideration of other variables and their different interdependencies. Thus, in addition to the SWT parameter, the Ostergren and Zamrik damage parameters are newly considered in the prediction.

Parameter SWT

The SWT parameter is a classical damage parameter used mainly in the low-cycle isothermal fatigue. The parameter is constructed as a combination of stress amplitude, total strain and elastic modulus according to (1).

$$P_{SWT} = \sqrt{\sigma_a \cdot \varepsilon_a \cdot E} \tag{1}$$

Regression analysis over the experimental data is able to be performed in various ways. A common way is to gain the P_{SWT} parameter by substituting regression relationships for each parameter element. Substituting the equations σ_a and ε_a showed in (2, 3) into (1) gives (4).

$$\sigma_a = \sigma_f'(2N)^b \tag{2}$$

$$\varepsilon_a = \frac{\sigma_a}{E} + \varepsilon_f'(2N)^c \tag{3}$$

$$P_{SWT} = \sqrt{\sigma_a \cdot \varepsilon_a \cdot E} = \sqrt{\sigma_f'(2N)^b \cdot E \cdot \left(\frac{\sigma_f'(2N)^b}{E} + \varepsilon_f'(2N)^c\right)} \tag{4}$$

Another method of using regression fitting of experimental data may be polynomial fitting according to formula (5). It is also used in the Ostergen and Zamrik damage models as shown below.

$$P_{SWT} = A(N)^B \tag{5}$$

Damage parameter based on Ostergren model

Another model of damage factor is model proposed by Ostergren in [7]. The model was used in [8] and [9]. The main parameters of the model are the tensile part of inelastic hysteresis energy and cycling frequency. According to [8], the model was used by combination of plastic deformation amplitude and the maximum stress as shown in Eq. (6).

$$P_{OST} = \Delta\varepsilon^{pl} \cdot \sigma_{max} \tag{6}$$

Regression analysis over the experimental data is usually performed to obtain regression coefficients as shown in Eq. (7).

$$A = N_f^B \cdot P_{OST} = N_f^B \cdot \Delta\varepsilon^{pl} \cdot \sigma_{max} \tag{7}$$

Damage parameter based on Zamrik model

Zamrik proposed in his work [9] a modification of the Ostergren model by using the maximum tensile energy amplitude instead of the non-elastic energy amplitude, ie. by including the highest tensile stress and temperature, and by including or eliminating the effect of pressure strokes. The model can be expressed according to [9] in the form (8).

$$N_f = A(\Delta W)^B \cdot \big(h(t)\big)^C \cdot \big(r(T)\big)^D \tag{8}$$

In Eq. (8) ΔW represents an energy function, $h(t)$ represents a creep or environmental effect due to hold-time and $r(T)$ represents an elevated temperature effect.
Parameter of deformation energy amplitude ΔW can be expressed as the strain energy ratio during the fatigue test W_f and the deformation energy from the static test W_s. Parameter of amplitude of strain energy is then able to simplified to form (9) where the parameter is expressed as the dependence maximum stress, strain amplitude of tensile strain of the hysteresis loop in the middle of life, the strength limits and the extension of the static tensile test. The function of time-dependent phenomena is designed to take into account the effect of hold-time, as shown in Eq. (10).

$$\Delta W = \frac{W_f}{W_s} \approx \frac{\sigma_{max} \cdot \varepsilon_{ten}}{R_m \cdot A_f} \tag{9}$$

$$h(t) = 1 + \frac{t_h}{t_c} \tag{10}$$

Temperature-dependent parameters are included through activation energy to change the failure mechanisms. Temperature-dependent phenomena $r(T)$ are expressed by the Arhenius equation in the following Eq. (11)

$$r(T) = exp\left(\frac{-Q}{R(T_{max} - T_0)}\right) \tag{11}$$

The regression analysis over the experimental data is designed according to [9] to obtain the regression coefficients A and B in the form (12).

$$N = A(P_{ZAM})^B = A\left(\frac{\sigma_{max} \cdot \varepsilon_{ten}}{R_m \cdot A_f}\right)^B \tag{12}$$

Partial damage

Total damage consists of contributions from partial damage of various damage sources (mechanisms). In addition to the most significant type of mechanical fatigue damage caused by the cyclic change in plastic deformation, in particular in the case of thermally stressed parts, the further significant damage is the time-dependent effect of the temperature field. The stress under the influence of temperature induces in the components another damaging mechanism,

namely creep. However, the process assumes that mechanical fatigue is the main quantitative damaging effect.

The Prandtl-Ishlinskii hysteresis model is predominantly used to determine damage from mechanical fatigue. Using the hysteresis model in case of damage, the impact from the previous load is introduced into the damage calculation at the current point of solution. This procedure was presented in [2].

Implementation of the prediction scheme into the TMF_PRED program

The following chapter describes the prediction software for the prediction of thermomechanical fatigue based on available knowledge of the issue. After running the program, the program runs sequentially along the axis illustrated in the following Fig. 1. The calculation can be divided into the preparation phase and the damage calculation itself.

In the first step, fatigue curves and cyclic deformation curves for individual temperatures are discretized. The following is the identification of the closed hysteresis loop to the solved point and then the determination of the increase in damage size of the solved point.

For the subsequent calculation part, the input is a mechanical temperature history of loading. Input stress is a set of incremental time values of stress and temperature distribution. The input can be either results from the FEM program, or input directly using MATLAB functions.

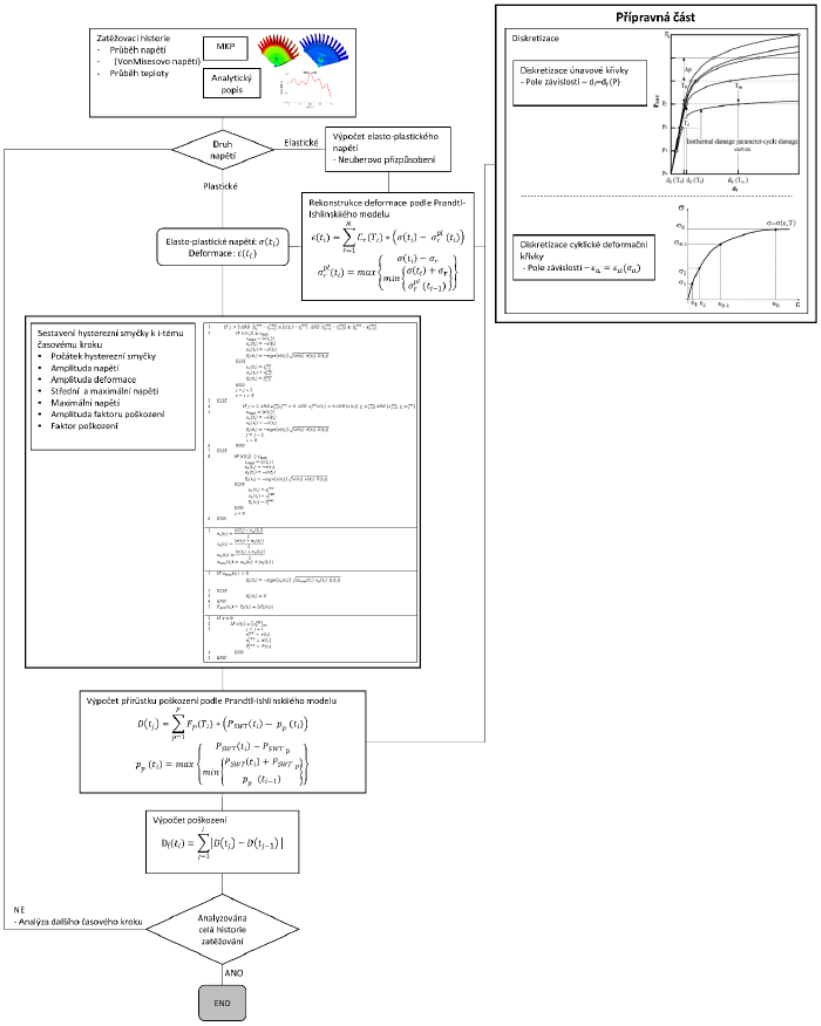

Fig. 1: TMF_PRED software scheme

Validation of a method of prediction thermo-mechanical fatigue and increase of damage

In the article [13], the results of damage calculation for the proposed basic stress spectra are published. It is a solution of combination of thermomechanical loading with variable temperature and stress. In the paper, it is possible to clearly distinguish values of individual peaks of stress and temperature of the load history. The 4 load histories listed in Table 5 are selected. The fatigue data of this material are taken from the article in graphical form of dependence $\sigma_a = \sigma_a(N)$. Values are used to correct the equivalent stress amplitude $\sigma_c = 360[MPa]$ for R=-1 and $\sigma_c = 305[MPa]$ for R=0.

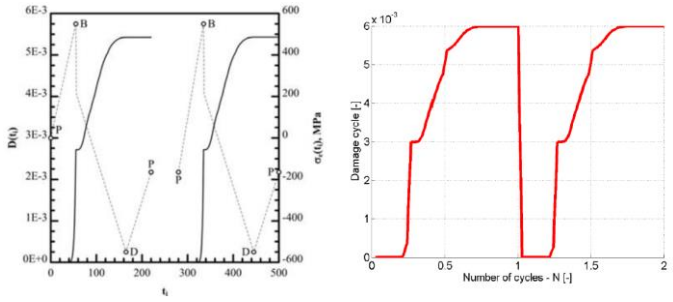

Fig. 2: Comparison of published results with the total damage for in-phase load (IP)

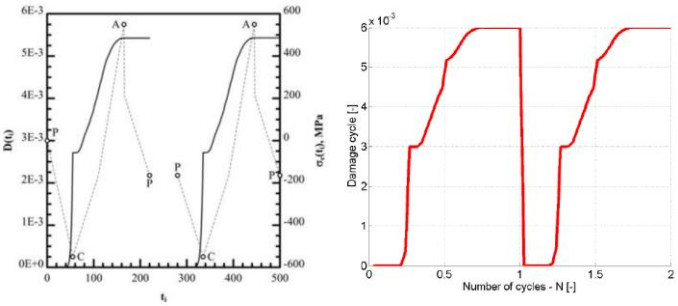

Fig. 3: Comparison of published results with total damage for out-phase load (OP)

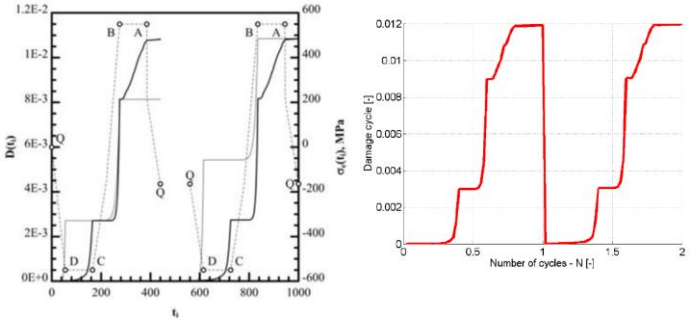

Fig. 4: Comparison of published results with total damage for thermo-mechanical cycling, ver. 1 ("clockwise")

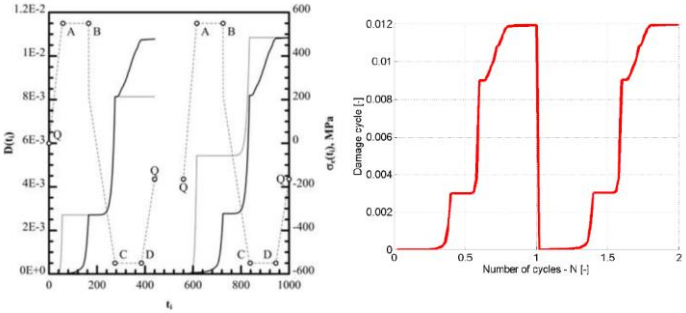

Fig. 5: P Comparison of published results with total damage for thermo-mechanical cycling, ver. 2 ("anti-clockwise")

Table 1 compares the published results ("PUB") and the results of the actual implementation ("PRED").

Table 1: Comparison of published results

Load history	Published result		Calculated result		Deviation $1 - \frac{PUB}{PRED}$	
	1. cycle	2. cycle	1. cycle	2. cycle	1. cycle	2. cycle
Load in-phase	5,427 E-03	5,431 E-03	5,994 E-03	5,998 E-03	9,5%	9,4%
Load out-phase	5,427 E-03	5,431 E-03	5,994 E-03	5,998 E-03	9,5%	9,4%
Cycling ver. 1	1,078 E-02	1,085 E-02	1,192 E-02	1,198 E-02	9,5%	9,5%
Cycling ver. 2	1,081 E-02	1,085 E-02	1,194 E-02	1,198 E-02	9,4%	9,5%

Aplication of experimental data

Measured data were compiled parameters of damage, according to the Eq. in Tab. 2. The SWT damage parameter was used based on the Eq. 4, the Ostergren damage parameter based on the Eq. 6, and the Zamrik model based on the Eq. 12.

In the case of Zamrik's model of damage parameter, the damage parameter in a simplified form Eq. 12 is used, since the loading did not contain hold-time according to experimental reports and the failure mechanism was not changed based on the results. The resulting summary of damage factors for each model is given in Table 4 below.

Table 2: Damage parameter summary

Name	**Model**	
SWT	$P_{SWT} = \sqrt{\sigma_a \cdot \varepsilon_a \cdot E}$	(4)
Ostergren	$P_{OST} = \Delta\varepsilon^{pl} \cdot \sigma_{max}$	(6)
Zamrik	$P_{ZAM} = \frac{\sigma_{max} \cdot \varepsilon_{ten}}{R_m \cdot A_f}$	(12)

The regression coefficients of the respective models were obtained by regression. Pair of regression coefficients for respective dependence were gradually determined by linear regression. Individual relationships and corresponding regression coefficients are summarized in Tab. 3. All fatigue models listed in Tab. 5 are expressed uniformly depending on the number of half cycles. The main reason is a uniform implementation of the damage calculation and a uniform approach to discretization of fatigue curves.

When processing regression dependencies in which plastic deformation occurs, the measurements usually do not take into account those measurements in which the magnitude of plastic deformation was less than a certain minimum value. This practice is related to the low accuracy of small plastic deformation determination. Usually the minimum value is used $\varepsilon_{0\,min} = 10^{-4}$.

Table 3: Fatigue models and regression coefficients

Model	Regression coefficients		
$\sigma_a = K'\left(\varepsilon_a^{pl}\right)^{n'}$	K'	n'	
$\varepsilon_a^{pl} = \varepsilon_f'\left(2N_f\right)^{c}$	ε_f'	c	(3)
$\sigma_a = \sigma_f'\left(2N_f\right)^{b}$	σ_f'	b	(2)
$P_{SWT\ IF\ const} = \sqrt{\sigma_f'(2N)^b \cdot E \cdot \left(\frac{\sigma_f'(2N)^b}{E} + \varepsilon_f'(2N)^c\right)}$	$\sigma_f', b, \varepsilon_f', c$		(4)
$P_{SWT\ POWER} = A_{SWT}\left(2N_f\right)^{B_{SWT}}$	A_{SWT}	B_{SWT}	(5)
$P_{OST} = A_{OST}\left(2N_f\right)^{B_{OST}}$	A_{OST}	B_{OST}	(6)
$P_{ZAM} = A_{ZAM}\left(2N_f\right)^{B_{ZAM}}$	A_{ZAM}	B_{ZAM}	(12)

Interleaving of material models according to Tab. 3 experimental data is shown in the following figures. Fig. 6 to Fig. 12 shows an example of model fitting with experimental data for T = 500 °C. The figures show the fit of the cyclic strain curve, Eq. 19, Manson-Coffin stress curve, Eq. 3, and the strain fatigue curve of the Basquin curve, see Eq. 2.

The course of the SWT damage factor, which is composed of the regression coefficients obtained from the deformation and fatigue curve according to Eq. 4, is shown in Fig. 9. The SWT parameter with power description according to Eq. 5 is shown in Fig. 10. The Ostergren model of the damage factor according to Eq. 6 is shown in Fig. 11, respectively. The Zamrik model of Eq. 12 is shown in Fig. 12.

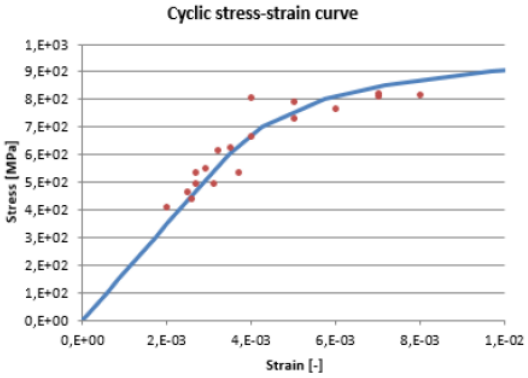

Fig. 6: Stress-strain curve, T=500°C

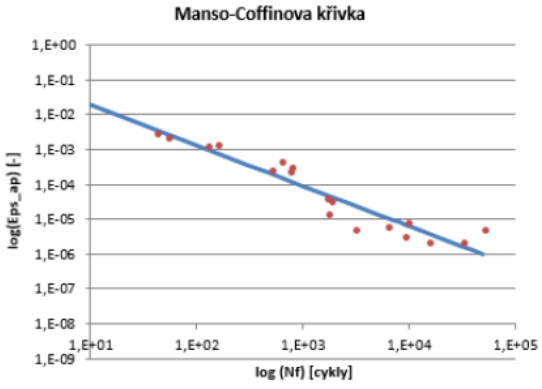

Fig. 7: Deformation fatigue curve, T=500°C

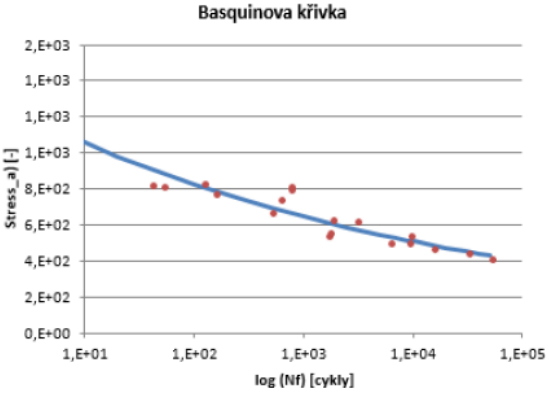

Fig. 8: Stress fatigue curve, T=500°C

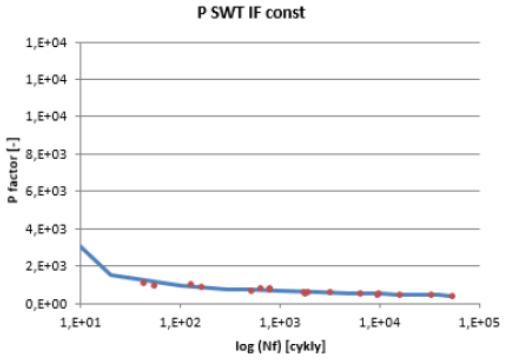

Fig. 9: SWT damage factor dependence on the number of cycles to failure, P factor composed of fatigue coefficients, T=500°C

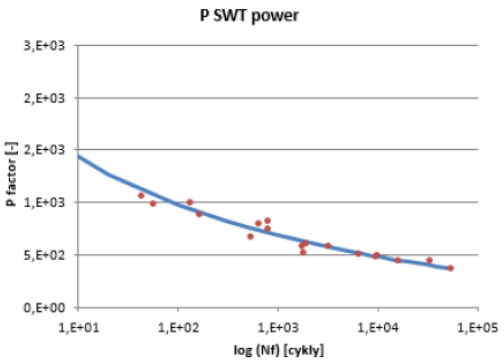

Fig. 10: SWT damage factor dependence on the number of cycles to failure, P factor composed of power model, T=500°C

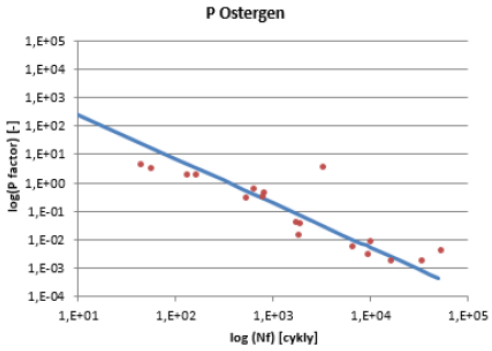

Fig.11: Ostergren damage factor dependence on the number of cycles to failure, T=500°C

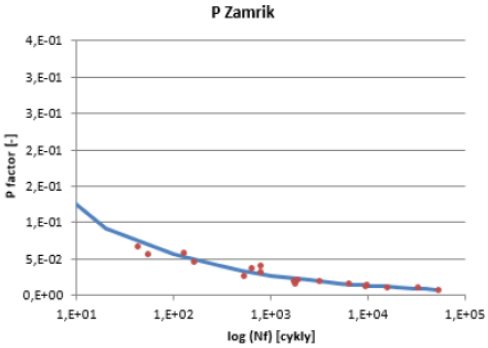

Fig.12: Zamrik damage factor dependence on the number of cycles to failure, T=500°C

In the figures, Fig. 13 to Fig. 19 is a comparison of cyclic strain curve, stress and strain fatigue curve, SWT, Ostergren and Zamrik damage factors for each processed temperature.

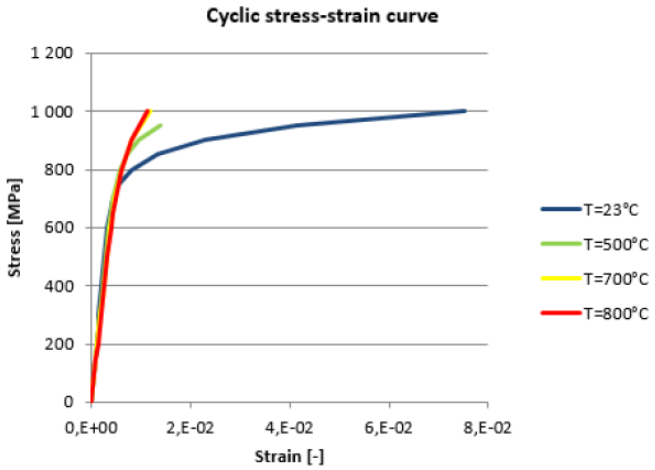

Fig. 13: Cyclic deformation curves for individual temperatures

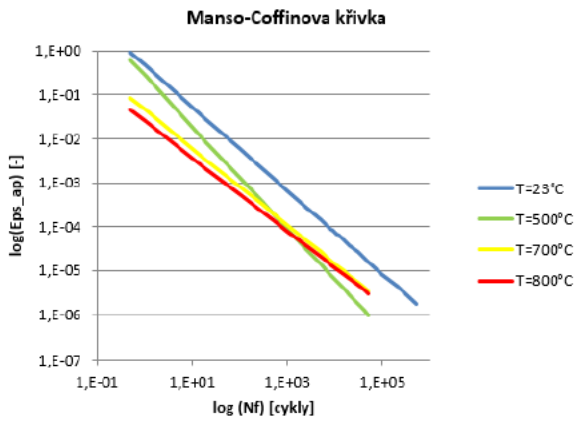

Fig.14: Deformation fatigue curves temperatures

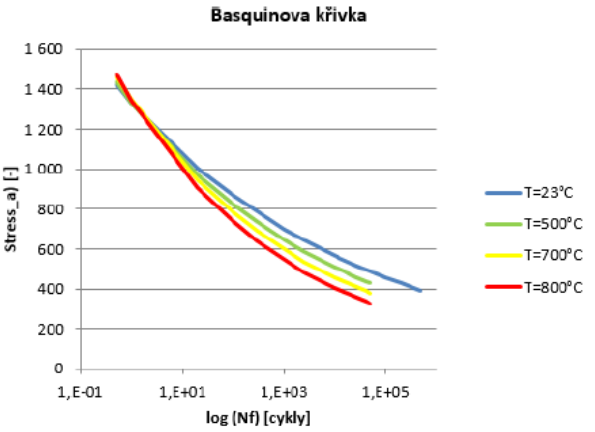

Fig.15: Stress fatigue curves according to according to temperatures

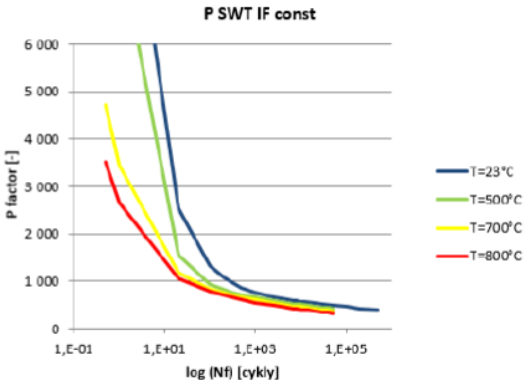

Fig.16: SWT damage factor depending on the number of failure cycles for individual temperatures, P factor based on fatigue coefficients

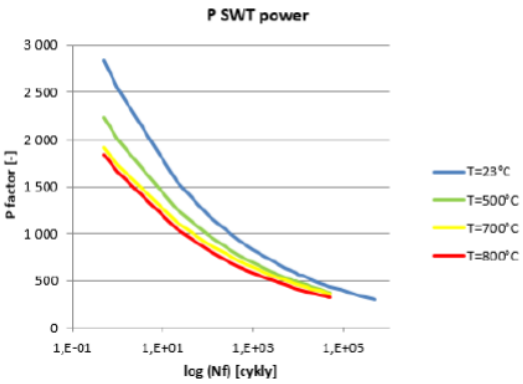

Fig.17: SWT damage factor depending on the number of failure cycles for individual temperatures, power model of P factor

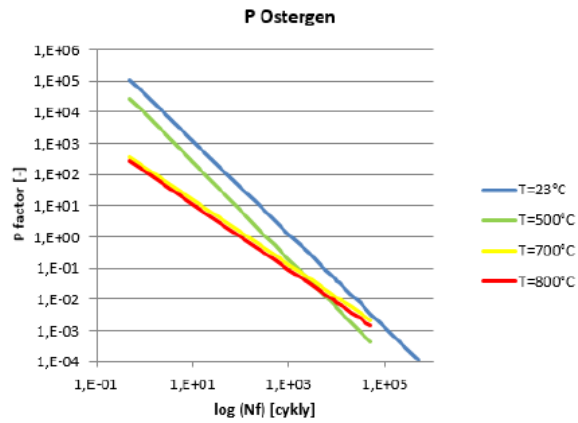

Fig.18: Ostergren damage factor depending on on the number of failure cycles for individual temperatures

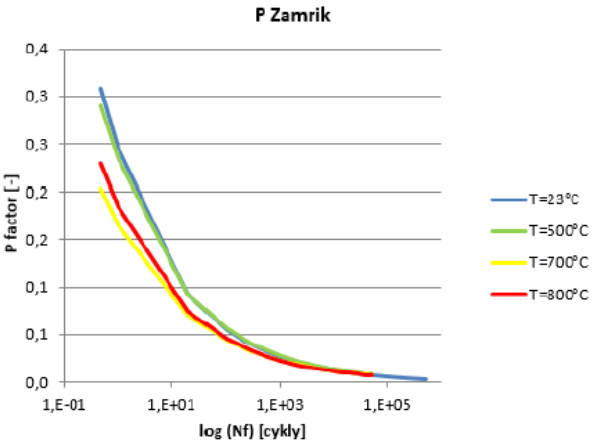

Fig.19: Zamrik damage factor depending the number of failure cycles for individual temperatures

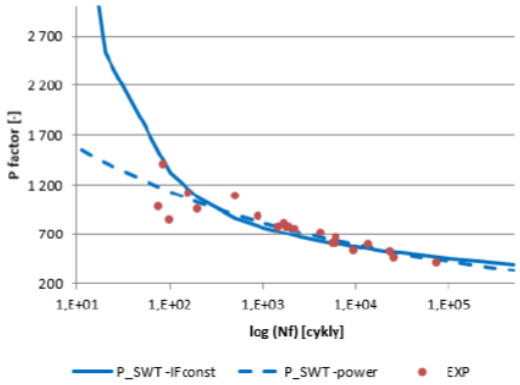

Fig.20: Comparison of SWT damage factor determined by fatigue coefficient and power model, temperature T = 23°C

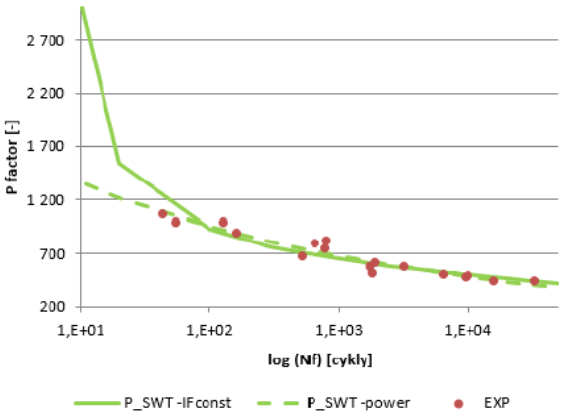

Fig.21: Comparison of SWT damage factor determined by fatigue coefficient and power model, temperature T = 500°C

A similar comparison for all temperatures is shown in Fig. 22. In this case, the biggest difference between the two ways of describing the SWT parameter is in the case of lower temperatures, namely T=23°C and 500°C. In the case of higher temperatures T=700°C and 800°C the difference is not so significant.

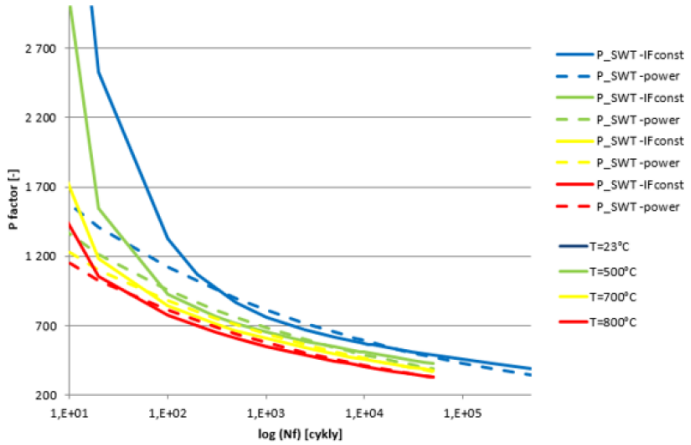

Fig. 22: Comparison of SWT damage factor determined by fatigue coefficients and power relations for individual temperatures

Conclusions

Damage parameters used for prediction of thermomechanical fatigue were presented in this paper. These methodologies are based on published sources and the object of the work was to compare input parameters and evaluate different results. TMF_PRED software for thermomechanical fatigue prediction was used to evaluate the output values. The whole prediction metodology is validated on the basis of available experimental data and based on published reports by prof. Nagodeho.

The damage parameter was compared in the SWT methodology in both the fatigue coefficient model (SWT IF const.) and the power relation (SWT power). Furthermore, the Ostergren methodology was compared and the last methodology was the Zamrik methodology. These methodologies were applied to experimental data where regression coefficients of the respective models were obtained to obtain uniform dependence on the number of half cycles.

Comparative CDK curves, stress and strain fatigue curves for individual temperatures were plotted for each methods. It can be seen from the graphs that the SWT method shows a

significant difference in the damage factor between models with fatigue coefficients and power eq. form. For the model with fatigue coefficients, the damage factor increases significantly with decreasing number of half cycles at low temperatures, at higher temperatures the growth is not so significant and the difference between the parameter of fatigue coefficient damage and power relation decreases with temperature. Furthermore, for all methods it can be stated that above 1e+3 half cycles there is no significant difference in the damage parameter with temperature, this fact corresponds to the fact that below this area, which is not the area of low-cycle fatigue and fatigue prediction is inappropriate.

It is also apparent from the comparison that the damage predicted by the SWT power factor described by the power eq. form (SWT power) is very close to the results of the Zamrik damage factor. In the case of the Ostergren factor, significantly less damage is predicted than other damage factors.

Based on the data presented in [6], where the fatigue life determined by the OP TMF is slightly longer than the IP TMF test, the difference between the prediction model and the test results is greater in higher cycles. This result shows that the Ostergren model is not suitable for predicting TMF life using isothermal fatigue test data. Zamrik modified the Ostergren model and developed a new model of life prediction for OP TMF.

Life predictions according to the Ostergren model are not effective in high cycle fatigue areas, life predictions according to the Zamrik model are more effective in these areas than according to Ostergren. It can also be seen that the Zamrik model is not suitable for predicting the life of an OP.

The main reason for the difference between the two prediction models is to incorporate the amplitude of the elastic stress as part of the damage parameter in addition to the inelastic strain deformation. Unlike Zamrik's model, the Ostergren model does not include the elastic stress amplitude as part of the damage parameter. However, in the case of materials with high strength and limited ductility, such as nickel-based superalloys, the elastic stress amplitude is significant, and therefore the elastic stress amplitude should be considered for TMF life predictions. In addition, the amplitudes of the inelastic deformations of LCF and TMF are small, and therefore small measurement errors and process utilization can cause large errors in results.

Discussion

The paper demonstrated different course and dependence of damage factor results as a quantifier of key fatigue damage control variables in thermomechanical fatigue. The above mentioned relations show the difference of input parameters for individual methodologies and under variable conditions. This raises the question of the suitability of specific methodologies for specific conditions affecting fatigue behaviour and lifetime prediction. The influence of temperature, LCF and HCF assumption, stress loading and material characteristics should be considered as control parameters of these specific conditions.

For example, the graph shows the suitability of the Zamrik methodology under varying temperature conditions or with a higher number of cycles. It is also appropriate to consider the quality of conservative and non-conservative estimates. Based on the previously studied VZLU data, these comparisons suggest that the closest prediction of LCF was achieved using the SWT parameter constructed using the power relationship in the experimental isothermal campaigns tested. Using the Ostergren parameter, a non-conservative estimate was predicted on average. Using other parameters a conservative prediction is achieved. Moreover, in the case of the Ostergren parameter of damage, the cycle numbers are predicted with the greatest variance. The variations for the other damage parameters were comparable.

Acknowledgement

This work was supported by Výzkumný a zkušební letecký ústav, a.s. in the project dealing with TMF prediction, project IMotor.

References

[1] J. Had, Implementation of interacting creep and fatigue under thermo-mechanical loading. *Engineering mechanics 2017*. Svratka, Czech Republic, 23rd International Conference.

[2] J. Had, Modelling of thermo-mechanical fatigue on engine generator turbine. *Engineering mechanics 2016*. Svratka, Czech Republic, 22nd International Conference.

[3] M. Nagode, M. Fajdig, Coupled elastoplasticity and viscoplasticity under thermo-mechanical loading. Fatigue & Fracture of Engineering Materials & Structures. (2006) 510-519.

[4] M. Nagode, D. Šeruga, M. Hack, E. Hansenne, Damage Operator-Based Lifetime Calculation Under Thermomechanical Fatigue and Creep for Application on Uginox F12T EN 1.4512 Exhaust Downpipes Strainl. (2012) 198-207.

[5] M. Nagode, Continuous damage parameter calculation under thermo-mechanical random loading. MethodsX. (2014) 149-160.

[6] M. Nagode, M. Hack, M. Fajdiga, Low cycle thermo-mechanical fatigue: damage operator approach. Fatigue & Fracture of Engineering, Materials & Structures. (2010) 149-160.

[7] W. J. Ostergren, A Damage Function and Associated Failure Equations for Predicting Hold Time and Frequency Effects in Elevated Temperature, Low Cycle Fatigue. Journal of Testing and Evaluation, (1976) 327–339.

[8] D. Lee, J. Lee, Y. Kim, J. M. Koo, C. S. Seok, Y. J. Kim, Thermo-mechanical fatigue life prediction of Ni-based superalloy IN738LC. International Journal of Precision Engineering and Manufacturing, 18(4), (2017) 561-566.

[9] S. Y. Zamrik, M. L. Renauld, Thermo-Mechanical Out-of-Phase Fatigue Life of Overlay Coated IN-738LC Gas Turbine Material. ASTM Special Technical Publication, 1371, (2000) 119–137.

[10] D. Holländer, D. Kulawinski, M. Thiele, C. Damm, S. Henkel, H. Biermann, U. Gampe, Investigation of isothermal and thermo-mechanical fatigue behaviour of the nickel-base superalloy IN738LC using standardized and advanced test methods. Materials Science and Engineering: A, 670, (2016) 314-324.

[11] D. Lee, I. Shin, Y. Kim, J. M. Koo, C. S. Seok, A study on thermo mechanical fatigue life prediction of Ni-base superalloy. International Journal of Fatigue, (2014) 62, 62-66.

[12] E. L. Robinson, Effect of temperature variation on the long-time rupture strength of steels. Trans. Am. Soc. Metals, (1952) 74, 777-781.

[13] M. Nagode, M. Hack, M. Fajdiga, High cycle thermo-mechanical fatigue: Damage operator approach. Fatigue and Fracture of Engineering Materials and Structure. 32.6 (2009) 505-514